NASA

TECHNICAL NOTE
D-1210

MEASUREMENTS OF MOMENTUM TRANSFER FROM PLASTIC PROJECTILES TO MASSIVE ALUMINUM TARGETS AT SPEEDS UP TO 25,600 FEET PER SECOND

By B. Pat Denardo

Ames Research Center
Moffett Field, Calif.

NATIONAL AERONAUTICS AND SPACE ADMINISTRATION
WASHINGTON
March 1962

E

NATIONAL AERONAUTICS AND SPACE ADMINISTRATION

TECHNICAL NOTE D-1210

MEASUREMENTS OF MOMENTUM TRANSFER FROM PLASTIC PROJECTILES TO MASSIVE ALUMINUM TARGETS AT SPEEDS UP TO 25,600 FEET PER SECOND

By B. Pat Denardo

SUMMARY

Momentum transfer during impact at speeds from essentially 0 to 25,600 feet per second was measured by a simple ballistic pendulum. The impacting projectile was made of linear high-density polyethylene and its shape and mass were maintained constant throughout the experiment. The impacted target was made of 2024-T4 aluminum. The resulting ratio of pendulum momentum to projectile momentum varied in an orderly fashion throughout the entire velocity range, reaching a minimum of 1.0 at about 3,000 feet per second and increasing to 1.9 at the highest velocity of 25,600 feet per second.

The change in mass of the target was also obtained, as were penetration data for this combination of materials. It was observed that the volume of the crater as measured directly was twice the volume of the crater as computed from the target mass loss at speeds above 10,000 ft/sec. Below 10,000 ft/sec this ratio increased rapidly with decreasing velocity.

During the course of this experiment some interesting features of impact were observed; namely, crater formation and ejected spray patterns. First, four distinct types of craters were discernible within the test velocity range. These changes in crater formation corresponded with noted variations in the momentum transferred to the pendulum. It was also noted that the ejected spray patterns showed a remarkable resemblance to the ray patterns emanating from certain craters on the Moon (e.g., Tycho, Kepler, and Copernicus).

INTRODUCTION

The ballistic pendulum was introduced to the scientific world in 1779 by Benjamin Thompson. Throughout the years the classical ballistic pendulum has changed very little. A block of material, such as wood, is suspended as a pendulum and a bullet is propelled from a gun into the block.

A scribe attached to the pendulum records the pendulum's motion. Knowing the mass of both the pendulum and the bullet, and transforming the pendulum's motion record into a velocity at impact, one may determine the velocity of the bullet at impact. The only assumptions required for this analysis are: the pendulum's motion is frictionless, the impact is inelastic, and the impact is direct and central.

The ballistic pendulum remains to this day, a simple instrument for measuring the velocity of a projectile, provided the impact is inelastic. However, if the mass and velocity at impact of both the projectile and pendulum are known, one may at once determine the apparent elasticity involved. To be more specific, the ballistic pendulum may be used to measure the momentum transfer when two bodies collide. It was this device, with only minor improvements, that was used to provide the measurements of momentum transfer at impact contained in this report. A 5 6 6

This research was instigated for several reasons. The most important was to investigate the nature of momentum interchange at impact as applied to piezoelectric impact detectors employed by experimental satellites. These sensors are used to give a measure, ultimately, of the mass of meteoritic dust particles and the collision frequency of these particles upon the satellite (refs. 1 and 2). While the present tests do not duplicate the conditions of hypervelocity impact encountered by the satellite and its impact detectors, namely, the size parameter and particle material, they do, however, extend nearly to the threshold of meteoric speeds. The data presented can be used to form a good engineering estimate of the response of impact detectors to hypervelocity impact.

During the past six years, much scientific research effort has been expended in the field of hypervelocity impact (e.g., refs. 3 and 4). A second purpose of the present study was to provide additional information on hypervelocity impact phenomena.

Data are presented in this report that depict the variation of the ratio of pendulum momentum to projectile momentum (a measure of the apparent elasticity of impact) with impact velocity, along with the variations of target mass loss, crater volume, and penetration with impact velocity. Also presented are pictorial displays of craters and resulting patterns of ejected spray.

SYMBOLS

A	sine wave amplitude, ft
D	diameter of crater, in.
d	model diameter, in.
g	acceleration due to gravity, ft/sec^2

l	length of pendulum arm, ft
M	weight of pendulum, lb
ΔM	target mass loss due to cratering, lb
m	weight of model, lb
P	penetration (depth of crater) measured from undisturbed surface, in.
T	time measured in pendulum motion, sec
$U_{measured}$	crater volume as measured directly, $in.^3$
$U_{computed}$	crater volume as computed from target mass loss, $in.^3$
V	velocity of pendulum at impact, ft/sec
v_f	velocity of model at impact, ft/sec
x	axial distance measured in pendulum motion, ft
τ	pendulum period, sec
φ	phase shift, radians

EXPERIMENTAL PROCEDURE

Description of Apparatus

This experiment was conducted in the Hypervelocity Ballistic Range of the Ames Research Center. Models were cylinders with spherical noses and were constructed of linear high-density polyethylene as shown in figure 1. Model shape, size, material, and, consequently, weight were maintained nominally constant throughout the tests.

The models were launched in free flight by means of a light-gas gun (ref. 5) at velocities above 10,000 ft/sec and by means of a standard 20-millimeter powder-gas gun at velocities between 1,500 and 10,000 ft/sec. Velocities below 1,500 ft/sec were obtained by means of a compressed-air chamber attached to the breech of the 20-mm powder gun.[1] The latter two means of launching the models were chosen instead of the light-gas gun, at their respective velocity ranges, mainly for simplicity.

[1]The data at a velocity of 11.5 ft/sec were obtained from a drop test and are included in table I.

Upon leaving the gun, the models flew through a series of small ports, through two spherical tanks, and then into a test chamber. This test chamber is a steel tube 8 feet in diameter and about 500 feet long. Spaced along the first 80 feet of the chamber are a series of eight spark shadowgraph stations. Six of these stations each record two right-angle views of the model; two stations record one view only. As the model flies through the chamber, it interrupts beams of light placed at each of these eight stations. A photocell sensor detects the passage of the model and induces a short-duration, high-intensity spark to discharge, exposing the shadowgraph film. At the instant this spark is discharged, a signal is fed into a counter chronograph. Thus, the position time history of the model's flight through the test chamber is recorded.

The ballistic pendulum was suspended at a distance of about 90 feet downrange (10 feet past the last spark shadowgraph station). This pendulum, as shown in figure 2, was simply a thin-walled steel tube suspended by the classical five-wire system. The target, made of 10- by 10- by 2-inch thick 2024-T4 aluminum, was securely attached to the front of the pendulum. Each target was backed up by a similar target to prevent spalling from the back of the test target at the higher velocities. The total weight of the pendulum could be varied to some extent to provide a suitably large swing at the lower velocities.[2]

To measure the position time history of the pendulum, a box containing five lamps was attached to the side of the pendulum and was viewed by a camera as shown in figure 3. Four of the lamps in this box were steady lights and one was a flashing light which flashed at precisely 60 cycles per second and was monitored by a time-interval counter. The length of time the various lamps were on and the sequence in which they were turned on were controlled by two wiper mercury droplet switches. These switches also started and stopped a series of counter chronographs which timed the period of the first four cycles of the pendulum. A reproduction of the 4- by 5-inch photographic glass plate of a typical test is shown in figure 4. The total swing of each of the first four successive cycles of the pendulum is given by the steady lights, and the initial velocity of the pendulum is derived from the flashing light.

Data Analysis

The following assumptions are made in analyzing the data of this report: (1) the motion of the pendulum is frictionless, and (2) the impact is direct and central. If these assumptions are valid, then the ratio of the pendulum momentum to the projectile momentum

$$MV/mv_f \qquad (1)$$

[2]At velocities below 1500 ft/sec, in order to obtain suitably large pendulum motions, it was necessary to construct a smaller pendulum.

indicates apparent elasticity effects in the form of model bounce, model splash, and crater material ejected, or combinations thereof, involved in the impact phenomenon.

The assumption of frictionless motion of the pendulum was checked by noting the maximum swing of the pendulum during four complete cycles after impact as recorded by the four steady lamps. A comparison of these swings indicated that the pendulum damping was approximately 1 percent per cycle.

The second assumption was that the impact was direct and central. The target was alined on boresight at a distance of about 90 feet from the muzzle of the gun. The maximum miss distance was 4 inches. If the model trajectory is assumed to be a straight line from muzzle to target, the resulting angle of obliquity is less than $1/4^{\circ}$, so that the impact may be considered direct. The center of gravity of the pendulum, in this case, was 4 inches off the line of impact, which definitely was not central. However, the swing of the pendulum was a smooth arc owing to its very large mass and five-wire suspension system; therefore, the impact may be considered central. The miss distance of 4 inches cited here was the maximum observed. The average miss distance for all tests was less than half this amount.

The weight of the pendulum, M, was measured before the test. The velocity of the pendulum at impact, V, was found by analyzing the time-distance history of the pendulum as recorded by the flashing lamp on the 4- by 5-inch photographic glass plate discussed in the previous section. The glass-plate data were read and recorded. A machine computer then fitted the raw data to a sine function,

$$x = A \sin(\sqrt{g/l}\, T + \varphi) \tag{2}$$

by the method of least squares. The constant, $\sqrt{g/l}$, was determined from the equation[3]

$$\tau = 2\pi/\sqrt{g/l} \tag{3}$$

where the period, τ, is the average of the four counter chronograph readings (see previous section).

The weight of the model, m, was determined prior to firing. It should be noted here that all high-velocity tests were performed at a chamber pressure of about 1-mm Hg. This was done to prevent any mass loss due to ablation of the model, since the calculations were based on

[3]The pendulum arm, l, was not measured directly and was not used in equation (2) for a number of reasons. First, it was basically more accurate to compute it from the pendulum period. Second, the length of pendulum arm varied slightly with pendulum weight. Third, it was felt that any abnormalities in the suspension system would be automatically accounted for this way.

the weight of the model prior to firing. Tests at lower velocities (less than 6,500 ft/sec) were performed at various chamber pressures in order to obtain proper velocities and better model stabilization. Mass loss of the model due to bore friction has been measured by other researchers at this Center (ref. 6). Based on this work, the polyethylene model used in this experiment would lose approximately 1 percent of its mass as a result of bore friction when launched by a light-gas gun at a velocity of 20,000 ft/sec. An analysis of all parameters involved indicates that in the determination of the momentum ratio this variation in the model weight controls the accuracy.

The velocity of the model at impact, v_f, was determined from the range data in the form of a plot of the reciprocal of the model velocity versus time (ref. 7). An extrapolation to the target is necessary but will not induce significant error, since it is located less than 10 feet from the last spark shadowgraph station.

DISCUSSION OF RESULTS

Momentum Transfer

A compilation of the pertinent data is presented in table I. A plot of both the momentum ratio, MV/mv_f, and the target mass loss due to cratering, $\Delta M/m$, against the velocity at impact is shown in figure 5. Here it can be seen that both quantities vary in an orderly fashion with v_f. The variation of pendulum momentum with projectile momentum is presented in figure 6.

For velocities of about 2,000 to 4,000 ft/sec the momentum imparted to the pendulum is the particle momentum. However, at the higher test velocities the momentum imparted increases more rapidly than the particle momentum, indicating that at meteoric velocities, dust sensors could very likely respond to the kinetic energy of the particle (ref. 8). The changes in slope of the curve in figure 6 deserve some comment. The first and second line segments intersect at a point corresponding to an impact velocity of 3,100 ft/sec. This marks the beginning of mass loss in the target and corresponds to a momentum ratio of nearly 1.0, the theoretical minimum barring penetration through the target. At this unique point, the impact is almost perfectly inelastic; that is, the projectile appears to be absorbed by the target. In reality, of course, it is not. Here the projectile does not rebound but flows nearly radially so as not to contribute to the initial momentum interchange at impact. The next two breaks in the curve occur at impact velocities of 10,400 and 19,000 ft/sec, respectively. As will be discussed in the following section, these velocities correspond closely to changes in crater formation and target mass loss. Figure 6(b) is the upper section of figure 6(a) plotted to a larger scale to illustrate these points better.

Cratering

The dimensionless penetration, P/d, is plotted against the impact velocity, v_f, in figure 7. The "knee" in the curve is attributed to a sudden change in cratering behavior which is apparent in figure 8. There appear here to be four basic cratering regimes. The first includes impact at low speeds up to about 10,000 ft/sec and is characterized by a smooth bottom and attached crater lip. In this regime, the penetration data should be a smooth function of velocity. The second regime sets in just above 10,000 ft/sec and extends to about 14,000 ft/sec. Here the crater bottom begins to show small pitting, increasing rapidly with increasing velocity. Here also, the crater lip has broken away in a tension failure. Transition to the next regime is observed to commence in the last two photographs of figure 8(b). A large piece of crater bottom was found on the range floor following round MS-142. The first of these photographs shows this piece in place, the second shows it removed. Since there is no apparent change in the slope of the momentum curve at this point, as seen in figure 6, this piece undoubtedly broke out of the crater and simply fell to the floor. From 14,000 to about 22,000 ft/sec, the crater bottom contains numerous large faceted pits. Since the penetration is measured to the bottom of these pits rather than to the bottom of the crater contour, one can understand the occurrence of the "knee" in the curve of figure 7. Above 22,000 ft/sec, these pits reduce in size and increase in number, returning the curve to its original trend. It is suspected that the occurrence of this "knee" is highly dependent on the scale of the experiment. In other words, had a much thicker target been used the "knee" may have shifted or been eliminated altogether at these velocities. Reducing the size of the projectile would have the same effect. Preliminary examination of craters produced by caliber .22 polyethylene projectiles in 2024-T4 aluminum targets does indeed bear out this supposition. It should be pointed out here that the targets used in this experiment were not sufficiently thick to be considered semi-infinite in this speed range. Therefore, the penetration shown may be slightly greater than one would obtain with true semi-infinitely thick targets.

Crater volume as a function of impact velocity is shown in figure 9. First a liquid was used to measure the volume of the crater ($U_{measured}$); next the volume of the crater was computed on the basis of target mass loss ($U_{computed}$). As can be seen the ratio of these parameters is about 2 for velocities above 10,000 ft/sec. By observing the targets, one can speculate that local deformation of the target material is the predominant variable involved. As pointed out in the previous paragraph, these targets cannot be considered semi-infinitely thick and part of the discrepancy in the volumes could be attributed to target bulge. Below 10,000 ft/sec the volume ratio increases rapidly with decreasing velocity. Here it is apparent, since the targets may be considered semi-infinitely thick, that the difference in crater volumes is due only to deformation of target material. Hence, it appears likely that the volume ratio will be a function of target material, specifically target strength.

A simple physical analogy can help explain this phenomenon. If one were to take a ball peen hammer and strike the aluminum target, a depression would be formed. The depression would have a measurable volume, but the weight of the target would remain unchanged.

This discussion points out the hazard of using the crater volume as a measure of the mass loss. Large discrepancies can be encountered, depending on the impact velocity, target strength, etc.

Ejected Spray

Some typical patterns of ejected spray are shown in the photographs of figure 10. These are photographs of 1/4-inch plywood sheets which were placed 17-3/4 inches in front of the pendulum. They were painted black and had a hole cut approximately on boresight to permit the model to pass through to the target. The surface shown, of course, is that which faced the target. Several interesting features are illustrated by these photographs. One outstanding aspect is the presence of a ray pattern in which the rays do not emanate from the point of impact. This result is particularly interesting because it may suggest an explanation for the fact that on the moon, rays do not emanate from the center of the crater, as shown in figure 11.

Another feature of interest is the eyelid effect and offset center of the basic spray pattern. (This circular pattern represents a concentration of ejected material.) These have been found to correlate with model angle of attack at impact. An examination of figure 10 shows that as the velocity of impact is increased, the diameter of the basic spray pattern is decreased. Actually, at the highest test velocities it was noted that much of the spray escaped through the hole and was found uprange. This indicates that the direction of the spray becomes more alined with the axis of the pendulum, resulting in an increased momentum exchange. To repeat, at low-impact velocities, the spray is ejected mainly radially, and the resulting axial velocity component is small; hence, a low MV/mv_f. At high-impact velocities, the spray is ejected mainly straight back, and the resulting axial velocity component is high; hence, a large MV/mv_f.

SUMMARY OF RESULTS

Impact momentum transfer has been determined over a velocity range from essentially 0 to 25,600 ft/sec by a simple ballistic pendulum. The model was a polyethylene spherical-nosed cylinder and the target was made of 2024-T4 aluminum. The ratio of pendulum to projectile momentum, which is a measure of the apparent elasticity of impact, varied throughout the

velocity range, reaching its highest value at the maximum test velocity. It appeared that this ratio would continue to increase with an increase in velocity.

Data were also determined for target mass loss due to cratering and penetration. These parameters varied smoothly with velocity except for a knee which appears in the plot of penetration versus velocity. This knee is due to a change in crater formation; that is, large faceted pits are noted in the bottom of the crater. It is suspected that this phenomenon may be highly dependent on the scale of the experiment.

Crater volume as measured by a liquid was twice the crater volume as computed from the target mass loss at speeds above 10,000 ft/sec. Below 10,000 ft/sec this ratio increased rapidly with decreasing speed. It is speculated that target strength will control this volume ratio.

An interesting similarity of the rays in the spray patterns to the rays present on the moon was noted.

Ames Research Center
National Aeronautics and Space Administration
Moffett Field, Calif., Dec. 28, 1961

REFERENCES

1. Dubin, Maurice: Meteoritic Dust Measured From Explorer I. Planetary and Space Science, vol. 2, no. 2/3, April 1960, pp. 121-129.

2. LaGow, H. E., and Alexander, W. M.: Recent Direct Measurements by Satellites of Cosmic Dust in the Vicinity of the Earth. NASA TN D-488, 1960.

3. Charters, A. C.: High-Speed Impact. Scientific American, vol. 203, no. 4, Oct. 1960, pp. 128-140.

4. Summers, James L., and Charters, A. C.: High-Speed Impact of Metal Projectiles in Targets of Various Materials. Proceedings of Third Symposium on Hypervelocity Impact, Chicago, vol. 1, Oct. 7-9, 1958.

5. Bioletti, Carlton, and Cunningham, Bernard E.: A Very High-Velocity Gun Employing a Shock-Compressed Light Gas. NASA TN D-307, 1960.

6. Savin, Raymond C., Gloria, Hermilo R., and Dahms, Richard G.: Ablative Properties of Thermoplastics Under Conditions Simulating Atmosphere Entry of Ballistic Missiles. NASA TM X-397, 1960.

7. Yee, Layton, Bailey, Harry E., and Woodward, Henry T.: Ballistic Range Measurements of Stagnation-Point Heat Transfer in Air and in Carbon Dioxide at Velocities Up to 18,000 Feet Per Second. NASA TN D-777, 1961.

8. Isakovitch, M. A., and Roy, N. A.: Acoustical Method for the Measurement of Mechanical Parameters of Meteorites. Jet Propulsion Laboratory, C.I.T., Translation no. 2, Artificial Earth Satellites, Sept. 4, 1959.

TABLE I.- SUMMARY OF PERTINENT DATA

Round number	M, lb	V, ft/sec	MV, $\frac{\text{ft-lb}}{\text{sec}}$	m, lb	v_f, ft/sec	mv_f, $\frac{\text{ft-lb}}{\text{sec}}$	$\frac{MV}{mv_f}$	ΔM, lb	$\frac{\Delta M}{m}$	$\frac{P}{d}$	$\frac{P}{D}$	$U_{measured}$, $in.^3$	$\frac{U_{measured}}{U_{computed}}$
MS-129	217.10	1.496	324.8	0.009448	20,390	192.6	1.686	0.1241	13.14	0.963	0.278	2.41	1.96
MS-131	217.52	1.233	268.2	.009168	18,325	168.0	1.596	.1081	11.79	.886	.264	1.77	1.65
MS-133	217.96	1.294	282.0	.008932	19,300	172.4	1.636	.1067	11.95	.923	.276	1.98	1.87
MS-134	217.66	1.272	276.9	.009254	18,750	173.5	1.596	.1015	10.97	.968	.290	1.83	1.83
MS-135	217.78	1.136	247.4	.009297	17,000	158.0	1.566	.0769	8.27	.827	.267	1.52	2.00
MS-136	217.76	1.056	230.0	.009393	15,925	149.6	1.537	.0711	7.57	.830	.285	1.46	2.07
MS-138	217.65	.7254	157.9	.009362	12,300	115.2	1.371	.0361	3.86	.495	.191	.763	2.14
MS-139	217.53	.5747	125.0	.009392	10,420	97.90	1.277	.0253	2.69	.410	.166	.58	2.3
MS-140	217.64	.9415	204.9	.009316	14,795	137.8	1.487	.0593	6.37	.805	.283	1.19	2.03
MS-141	217.56	.7462	162.3	.009384	12,415	116.5	1.393	.0371	3.95	.506	.191	.793	2.16
MS-142	217.53	.8118	176.6	.009286	13,120	121.8	1.450	.0475	5.12	.583	.215	.946	2.01
*MS-142	217.53	.8118	176.6	.009286	13,120	121.8	1.450	.0544	5.86	.921	.339	1.13	2.10
MS-143	217.73	1.300	283.0	.009273	18,930	175.5	1.612	.1052	11.34	.900	.270	1.92	1.85
MS-144	217.58	1.756	382.1	.009258	22,900	212.0	1.802	.1558	16.83	1.106	.298	2.84	1.84
MS-145	217.57	1.724	375.1	.009499	22,100	209.9	1.787	.1500	15.79	1.002	.270	2.71	1.83
MS-146	217.36	2.104	457.3	.009389	25,600	240.4	1.902	.1897	20.20	1.189	.301	3.66	1.95
MS-148	217.41	1.956	425.2	.009259	24,400	225.9	1.882	.1839	19.86	1.117	.292	3.36	1.85
P-131	130.99	.7534	98.69	.009081	8,665	78.69	1.254	.0059	.65	.319	.153	.37	6.4
P-132	130.83	.5997	78.46	.009139	7,020	64.16	1.223	.0034	.37	.239	.130	.21	6.2
P-133	130.67	.1265	16.53	.009158	1,740	15.93	1.038	.0000	.00	.009	---	---	---
P-134	130.62	.3177	41.50	.009148	4,345	39.75	1.044	.0001	.01	.101	.076	.061	60.
P-135	131.18	.5206	68.29	.009177	6,340	58.18	1.174	.0017	.19	.192	.112	.15	8.8
P-136	130.69	.4233	55.32	.009138	5,340	48.80	1.134	.0007	.08	.148	.101	.092	10.
P-137	130.15	.2763	35.96	.009126	3,855	35.18	1.022	.0001	.01	.081	.071	.03	30.
MA-11	8.23	.4066	3.35	.009104	290	2.64	1.27	---	---	---	---	---	---
MA-12	8.23	.2981	2.45	.009023	215	1.94	1.26	---	---	---	---	---	---
MA-13	8.23	.6471	5.33	.009122	510	4.65	1.15	---	---	---	---	---	---

Drop height = 24.75 in. ~ v_f = 11.52 ft/sec; bounce = 16.19 in. ~ MV/mv_f = 1.809

*With piece removed.

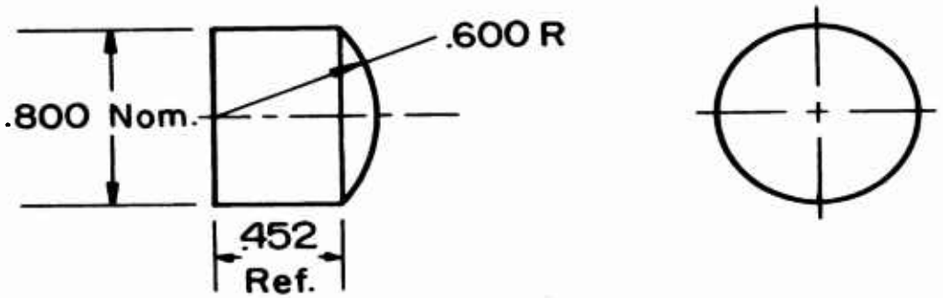

Dimensions in inches

Figure 1.- Model.

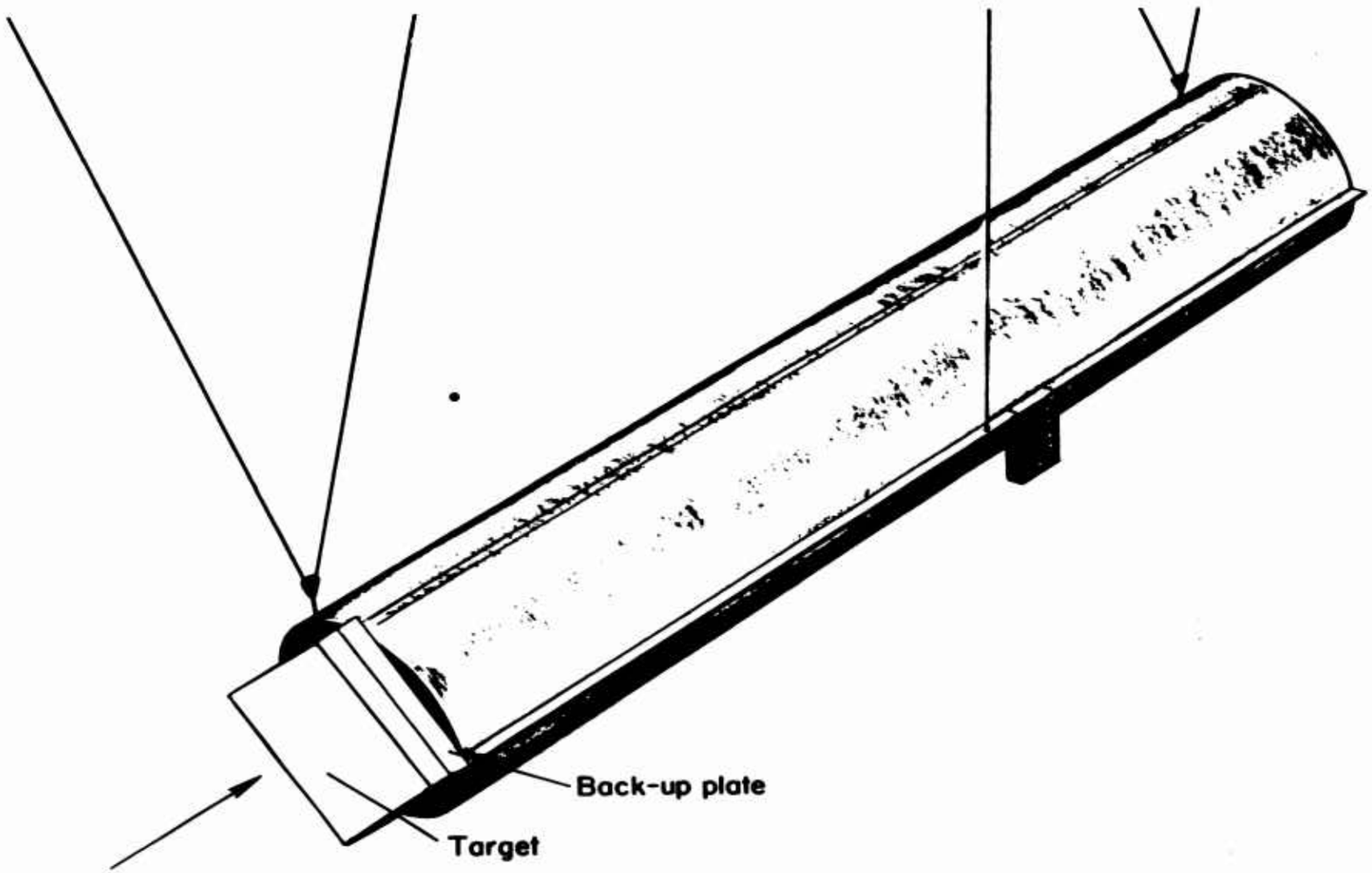

Figure 2.- Pendulum.

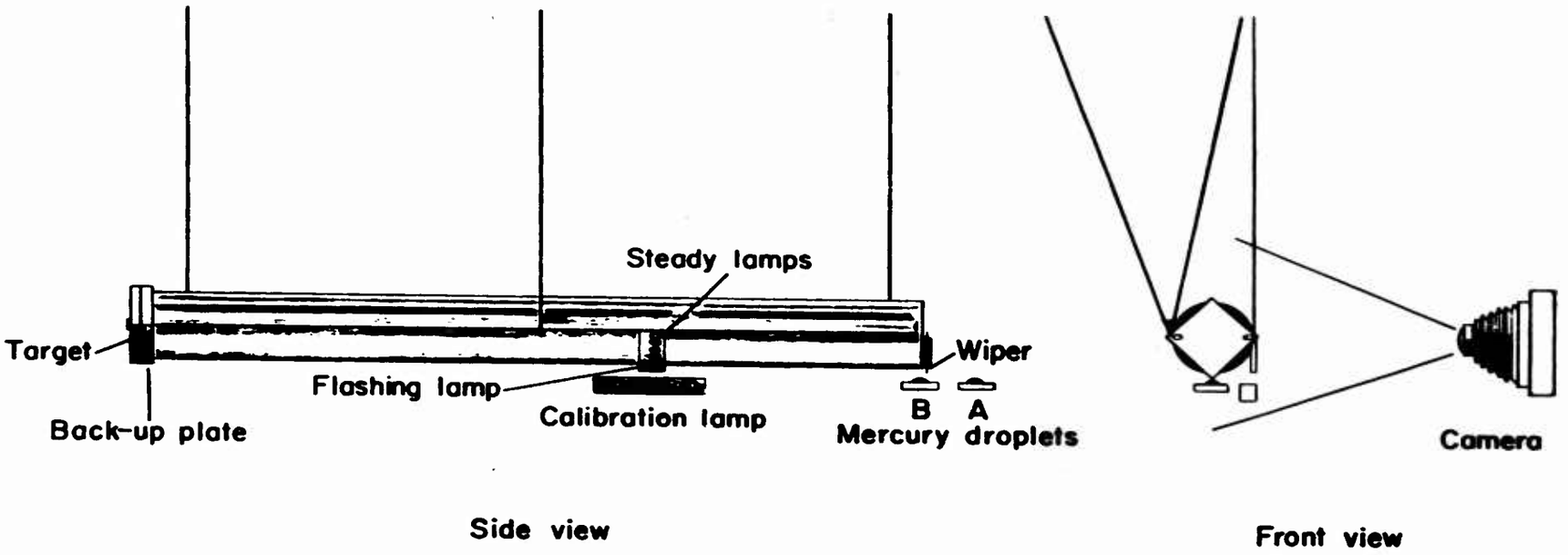

Figure 3.- Test setup.

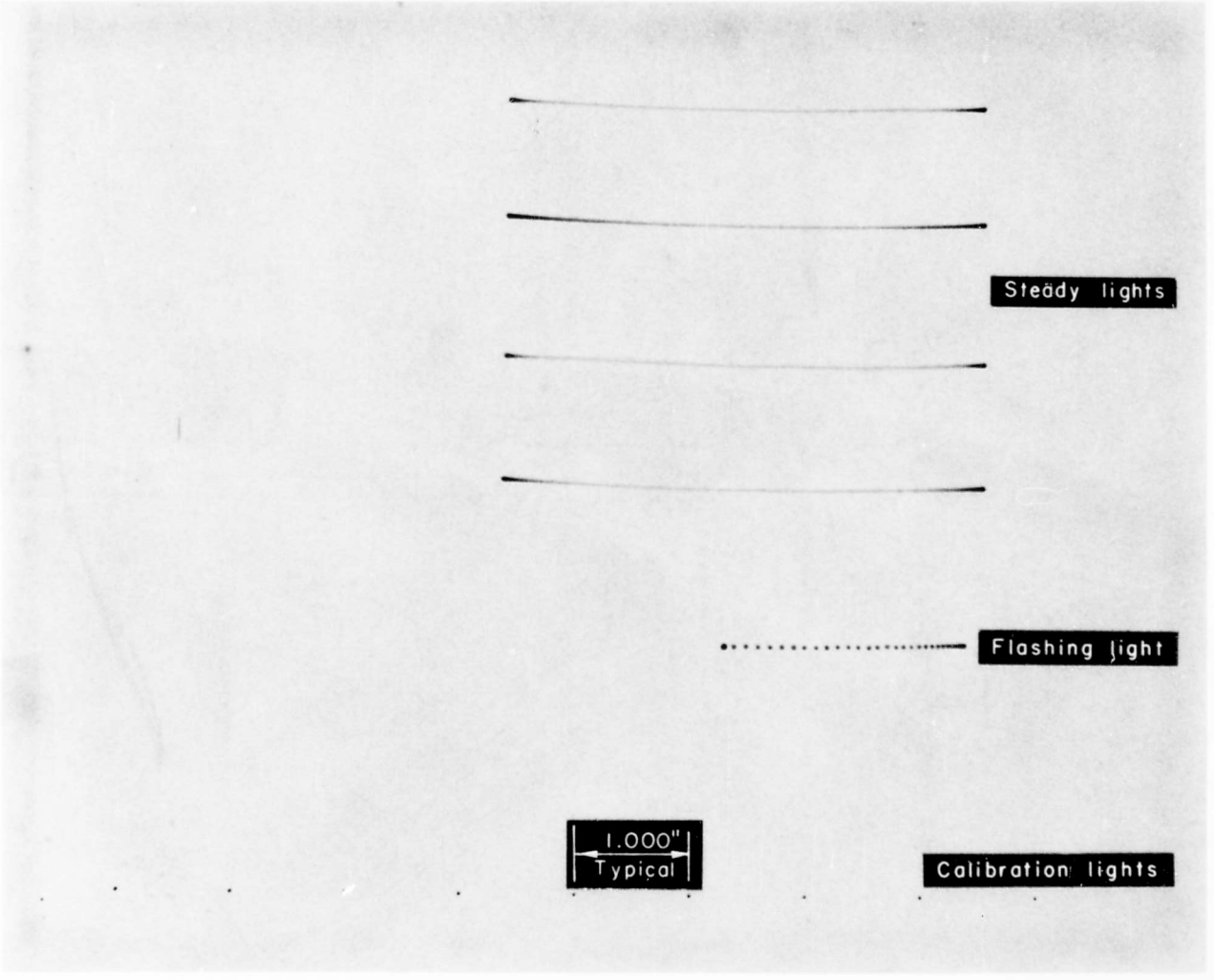

Figure 4.- Reproduction of 4- by 5-inch photographic glass plate (Round No. P-135).

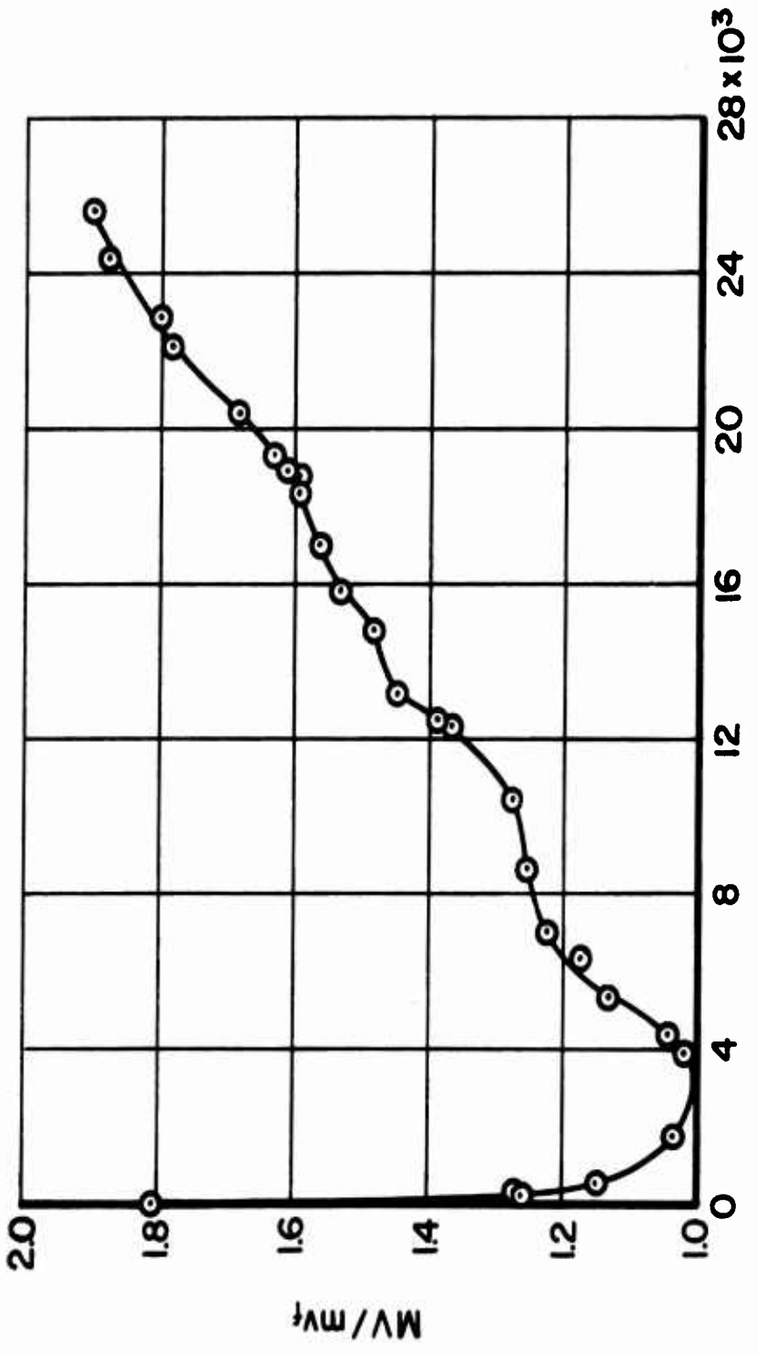

(a) Momentum ratio.

Figure 5.- Momentum ratio and target mass loss due to cratering as a function of impact velocity.

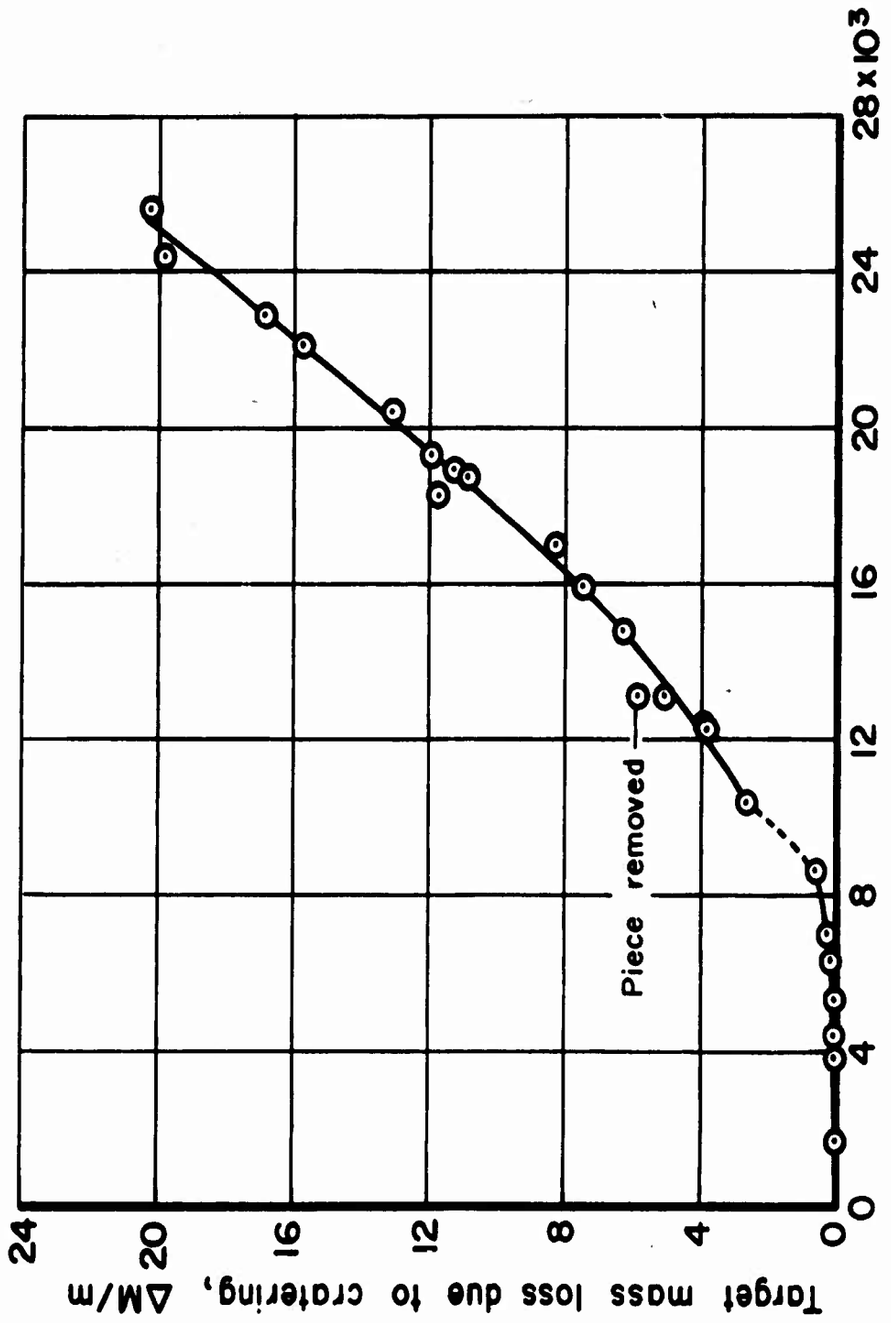

(b) Target mass loss due to cratering.

Figure 5.- Concluded.

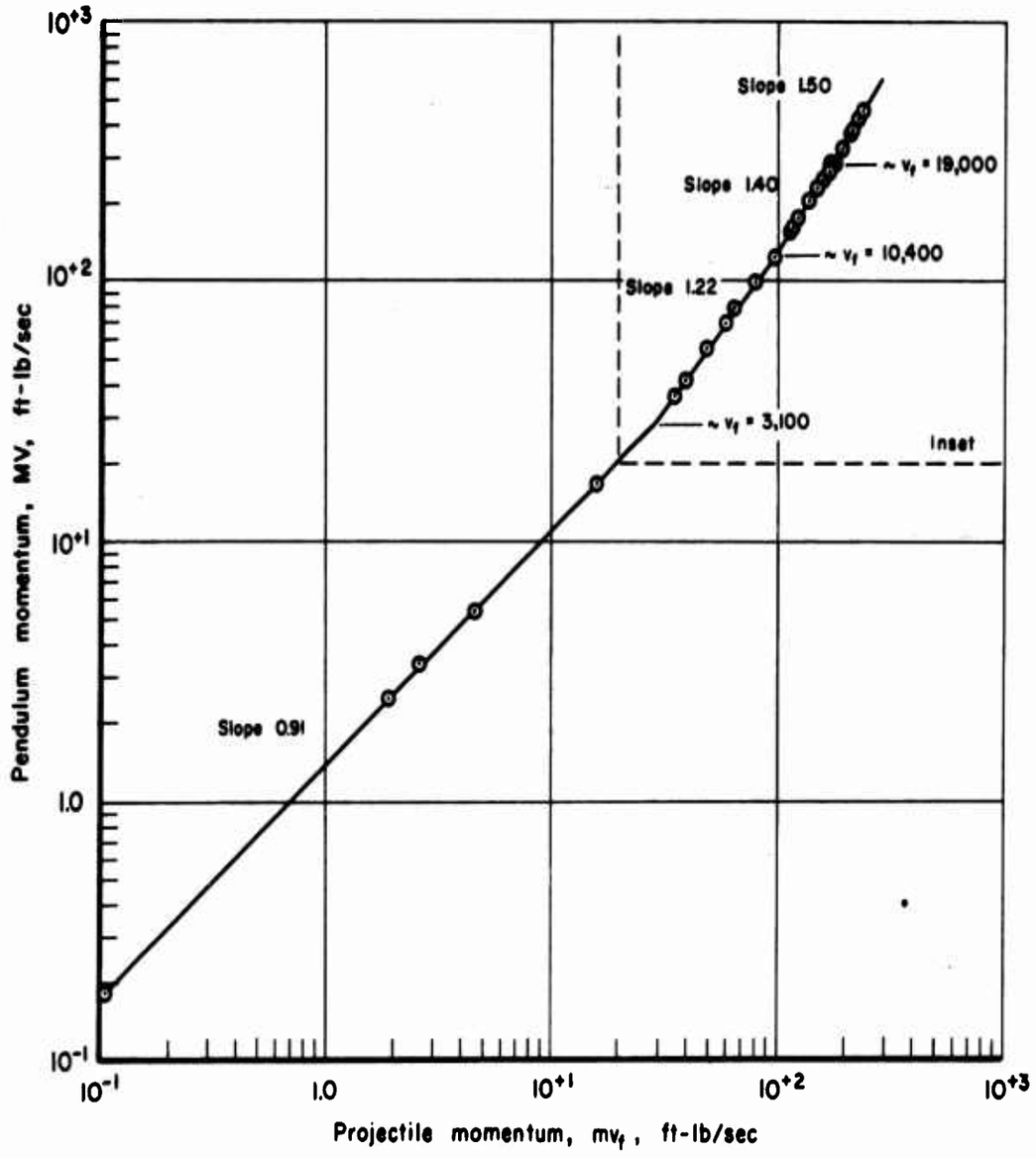

(a) Complete test range.

Figure 6.- Pendulum momentum versus projectile momentum.

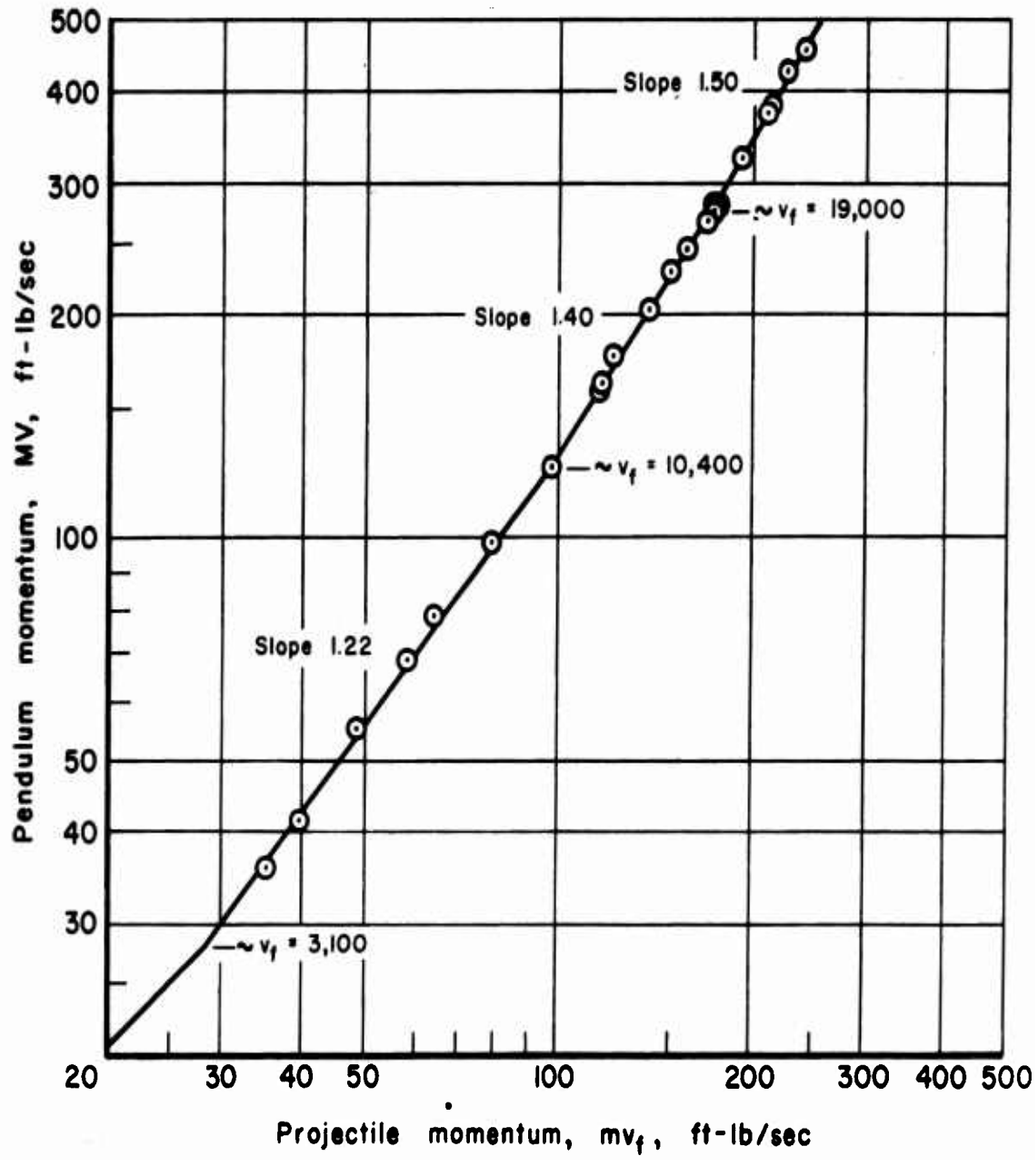

(b) Inset (enlarged).

Figure 6.- Concluded.

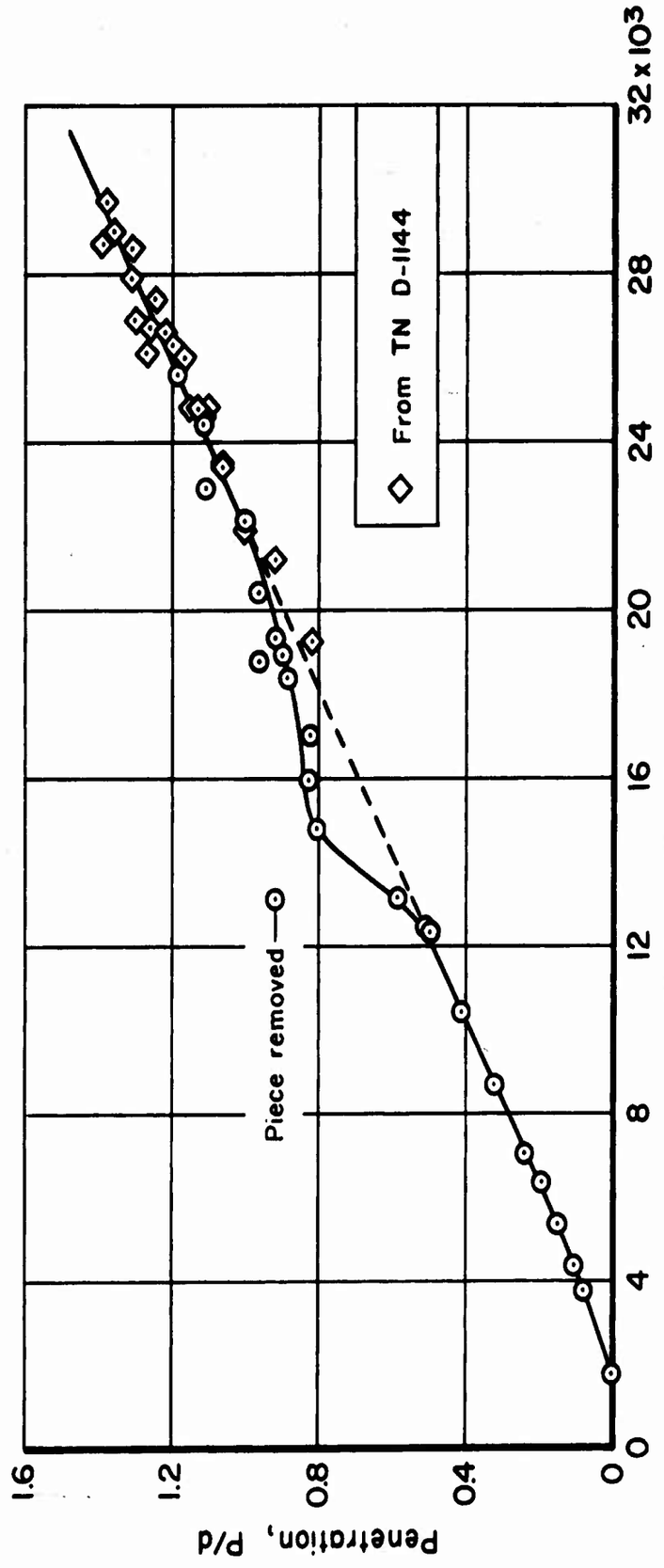

Figure 7.- Penetration versus impact velocity.

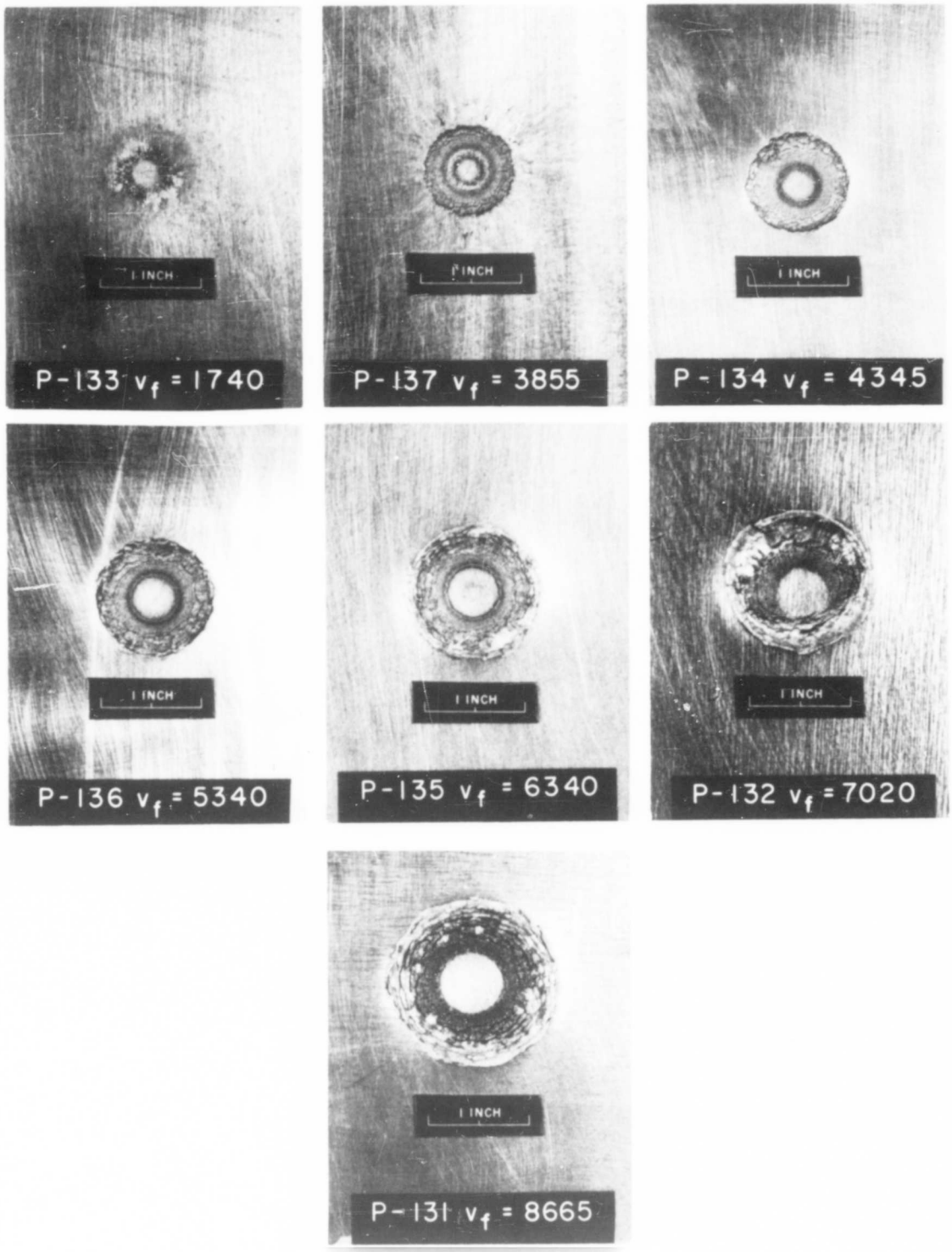

(a) First regime.

Figure 8.- Impact craters.

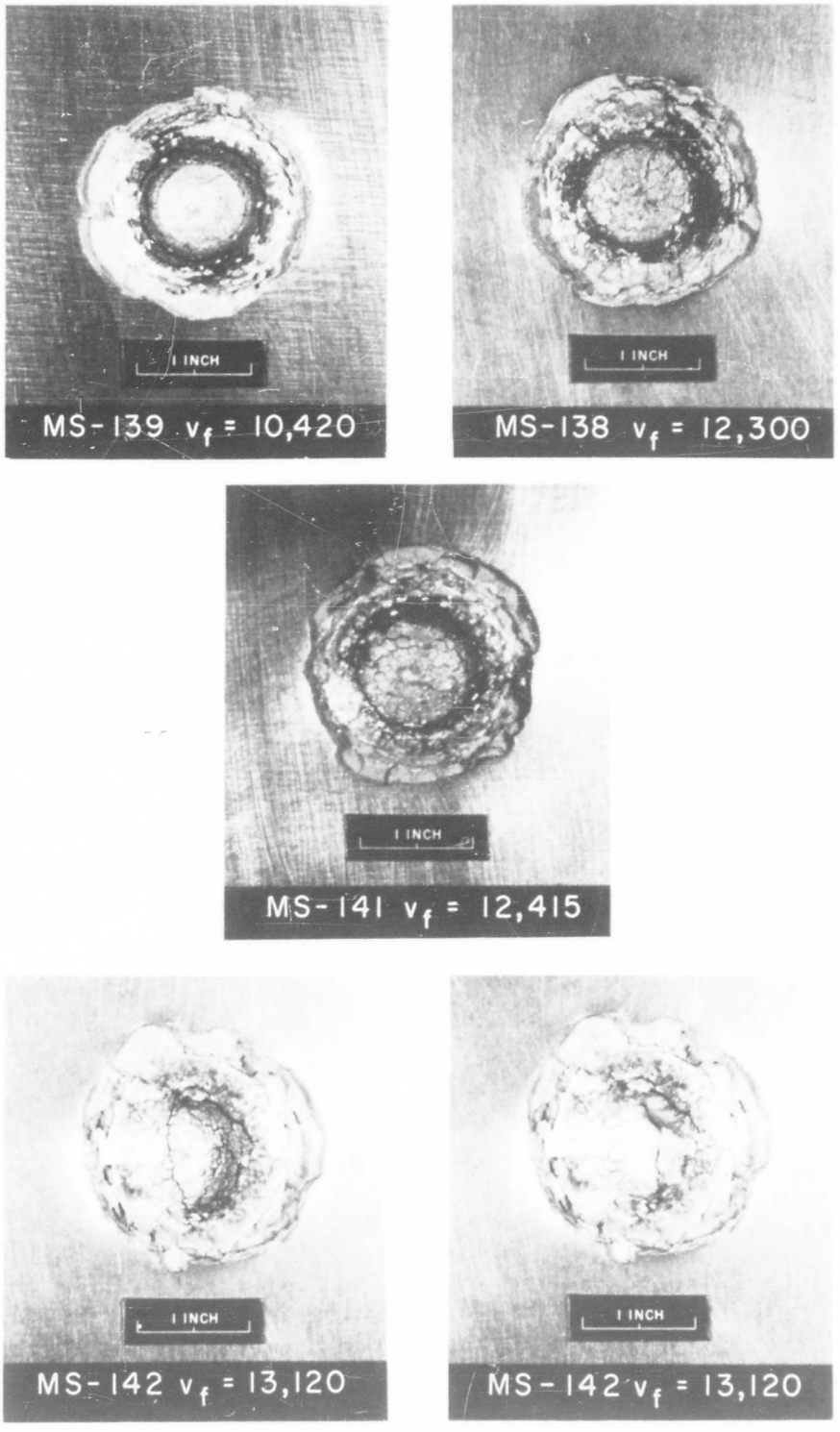

(b) Second regime.

Figure 8.- Continued.

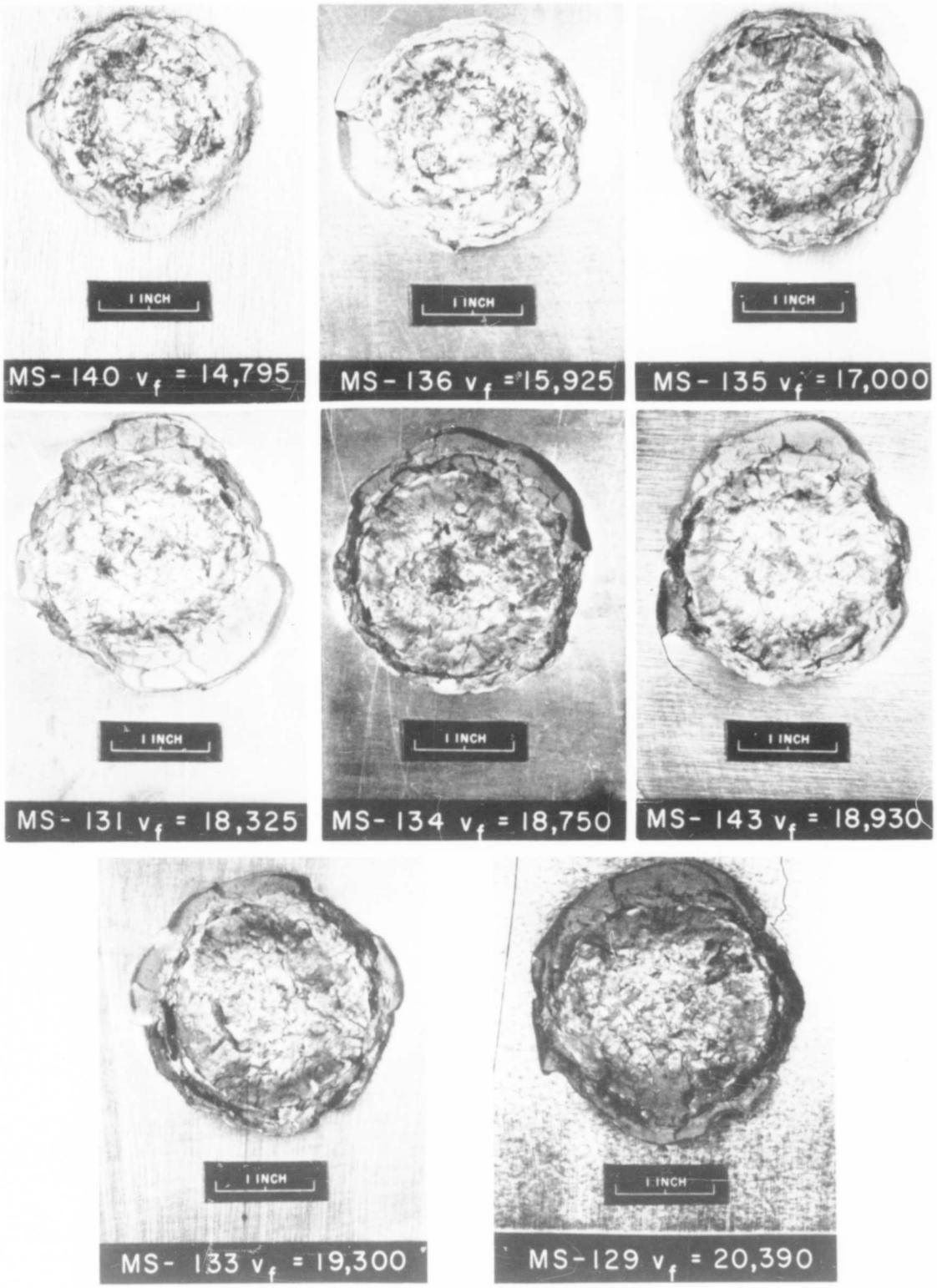

(c) Third regime.

Figure 8.- Continued.

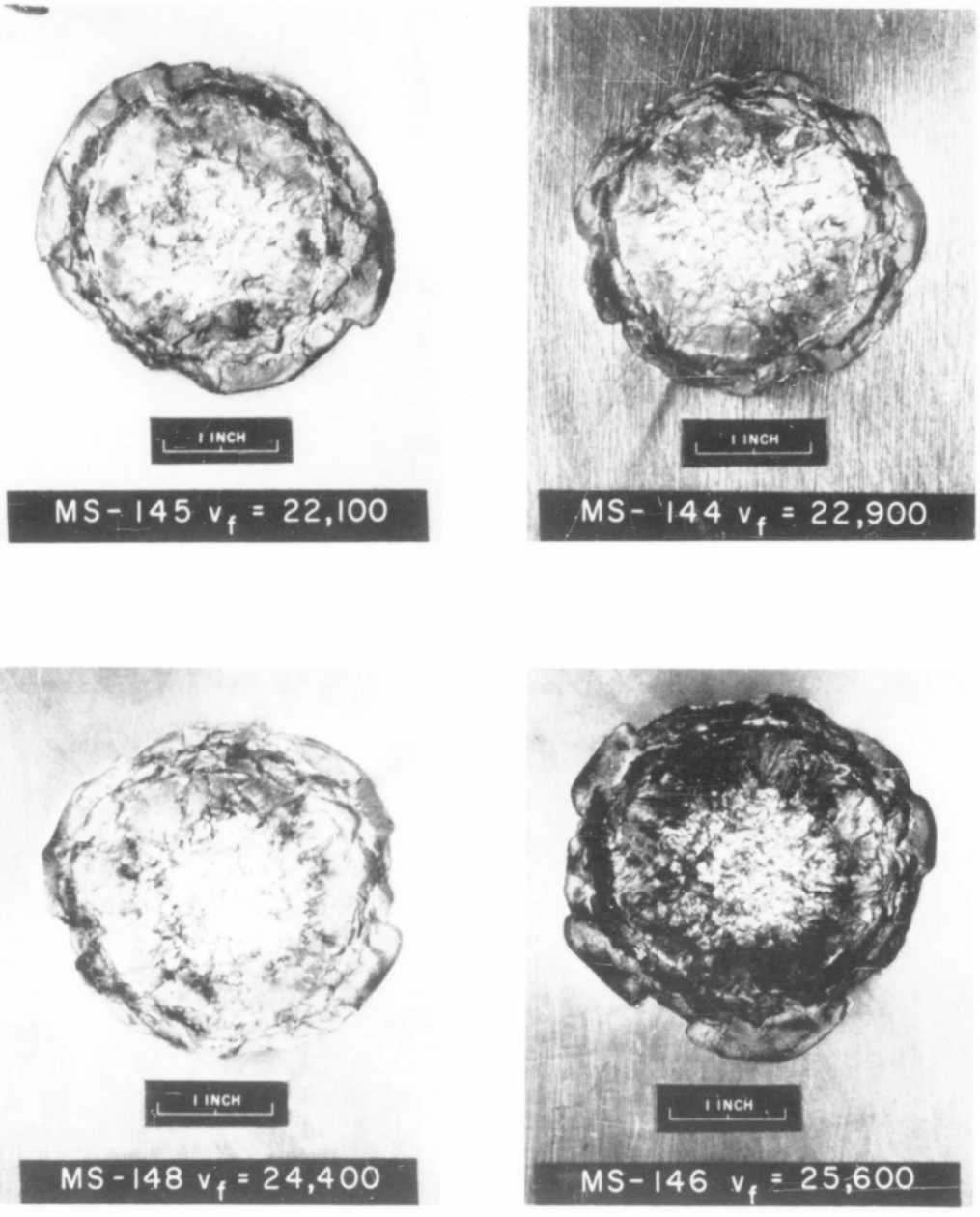

(d) Fourth regime.

Figure 8.- Concluded.

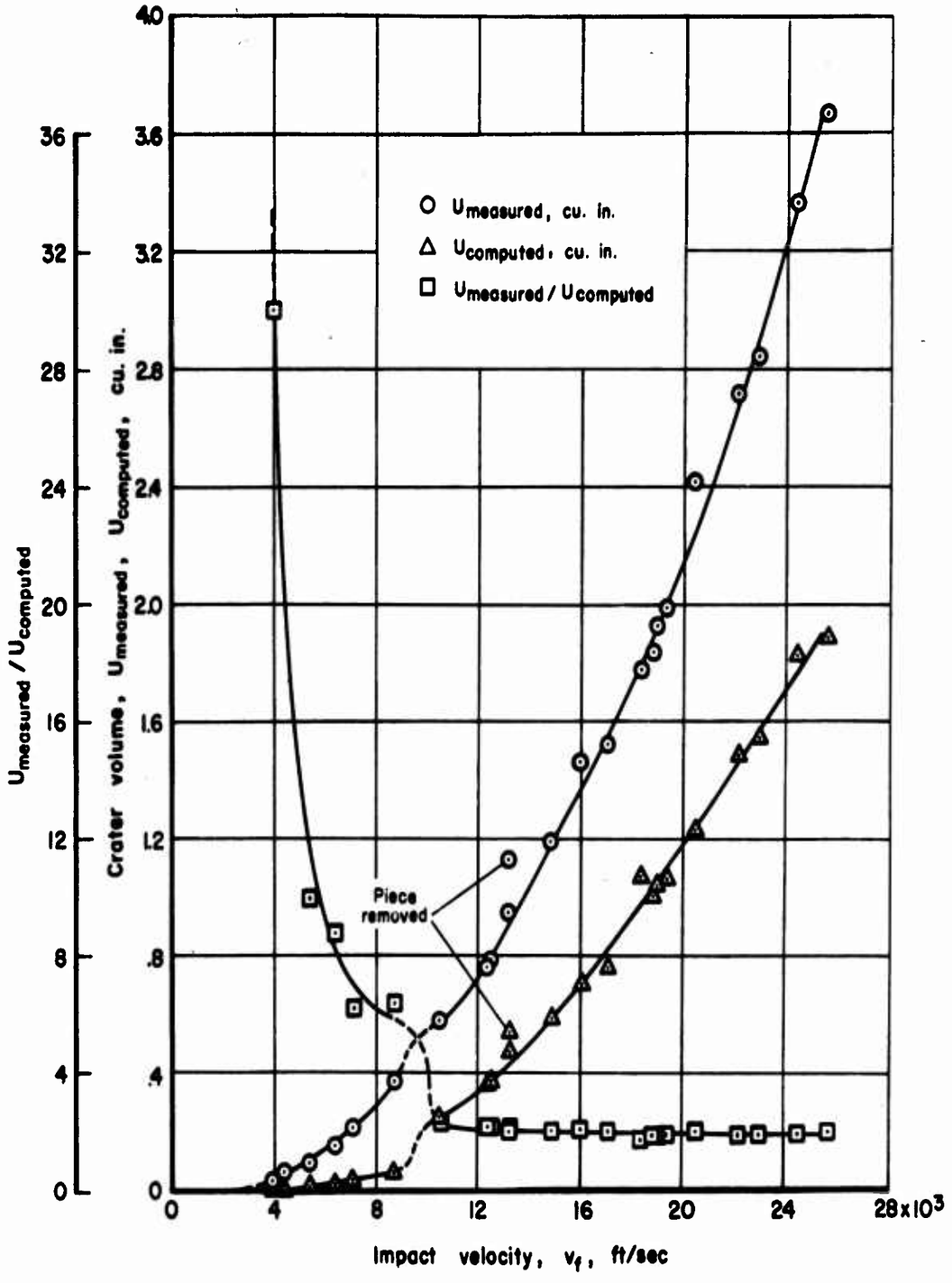

Figure 9.- Crater volume as a function of impact velocity.

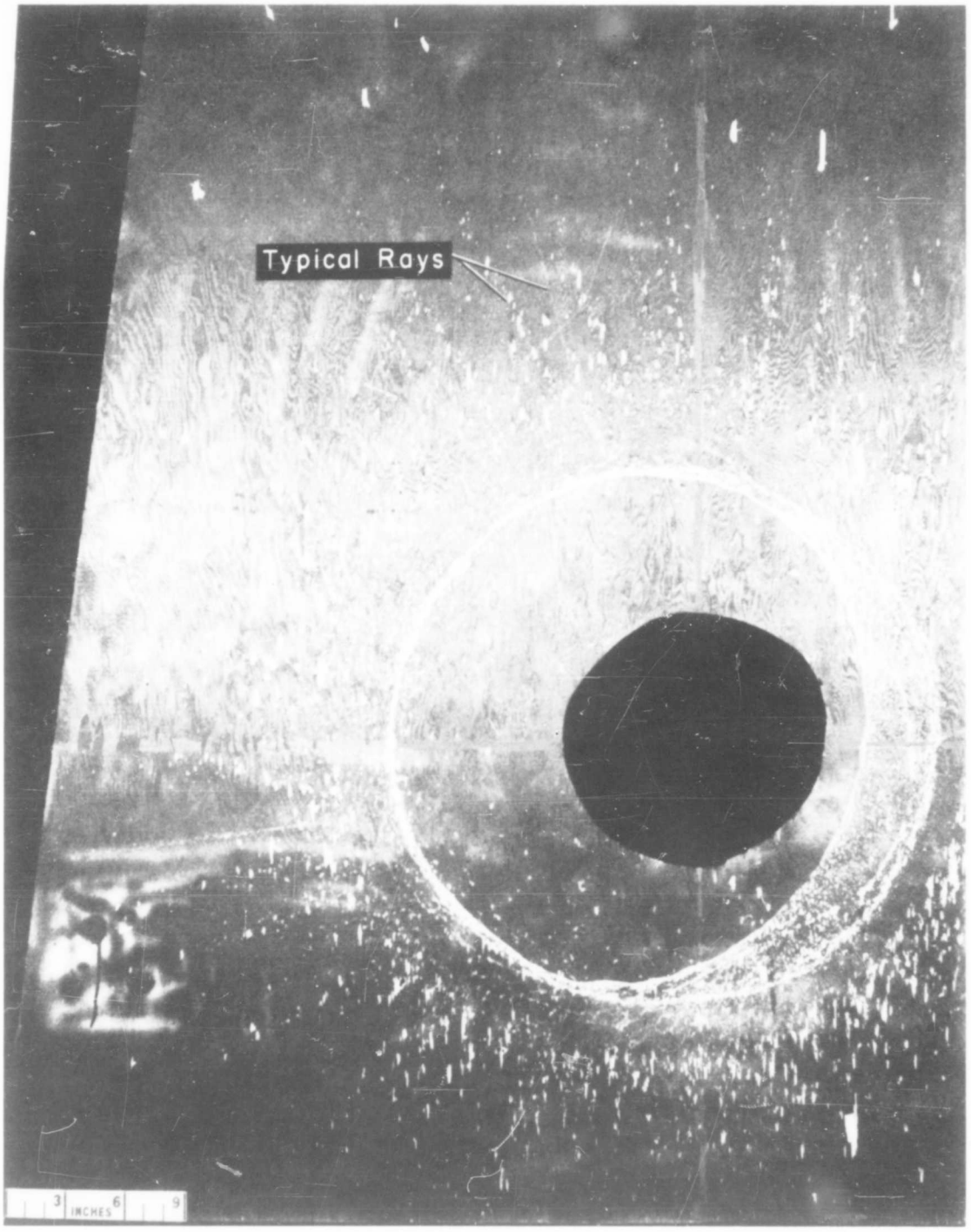

MS-135 v_f = 17,000

Figure 10.- Ejected spray patterns.

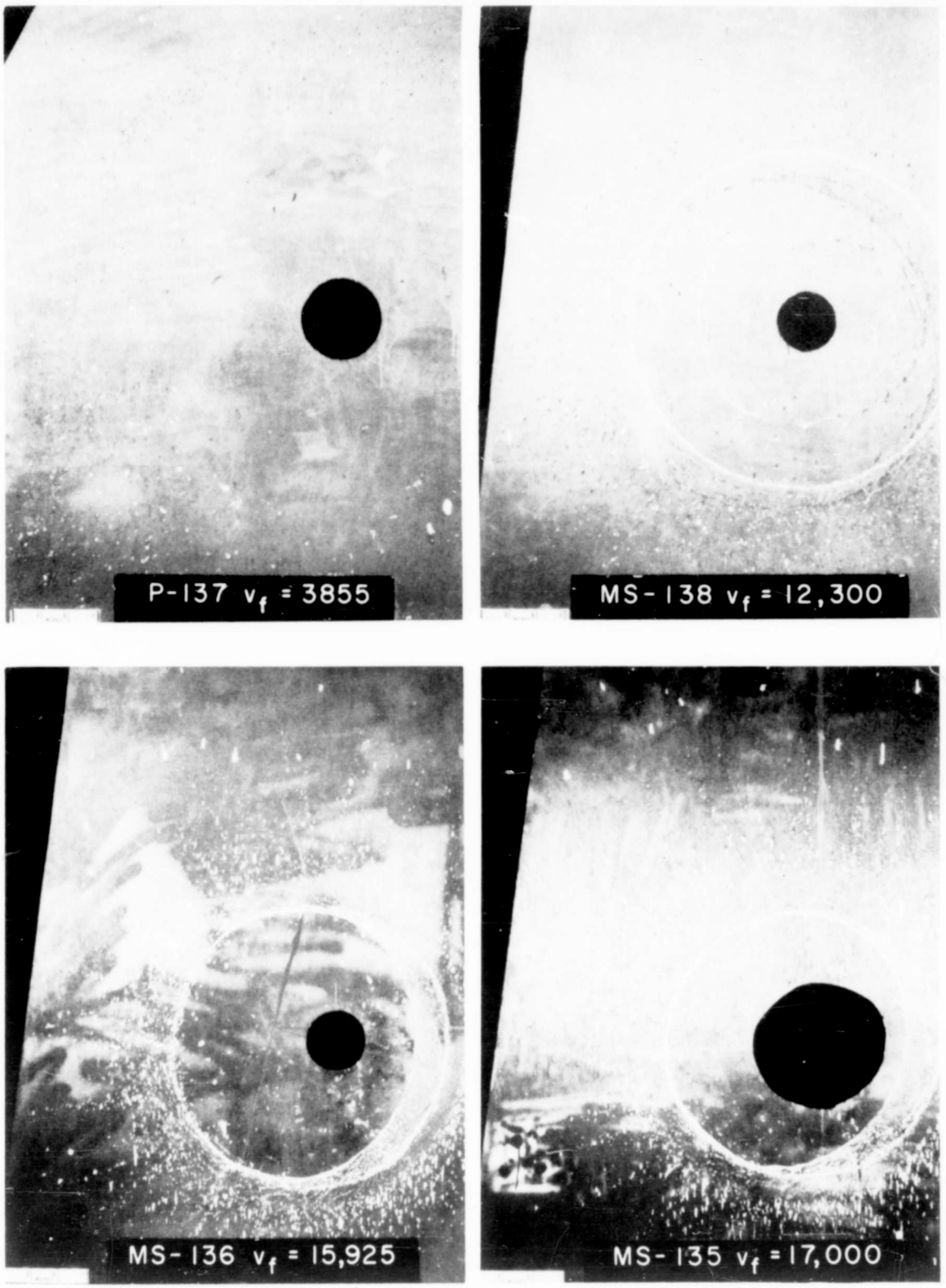

Figure 10.- Continued.

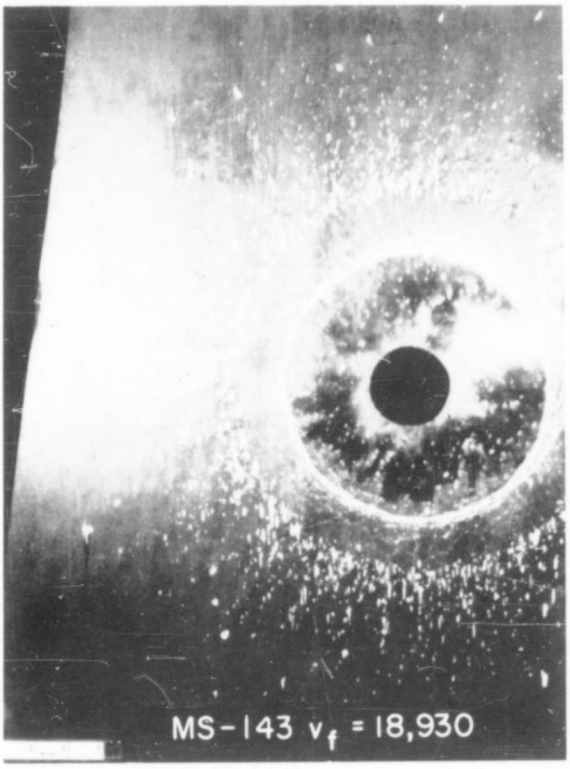

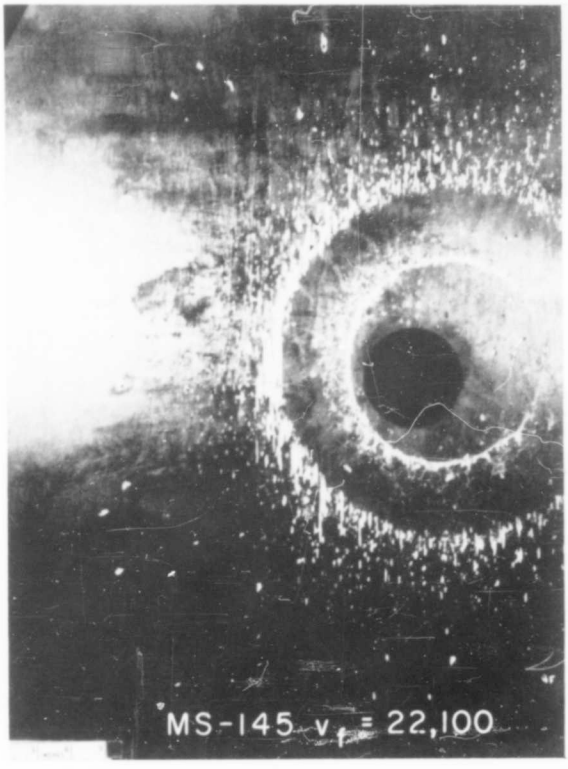

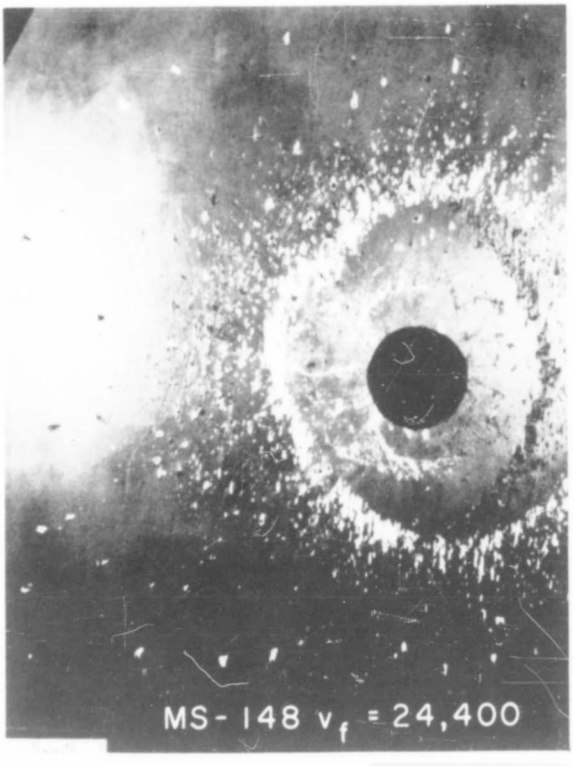

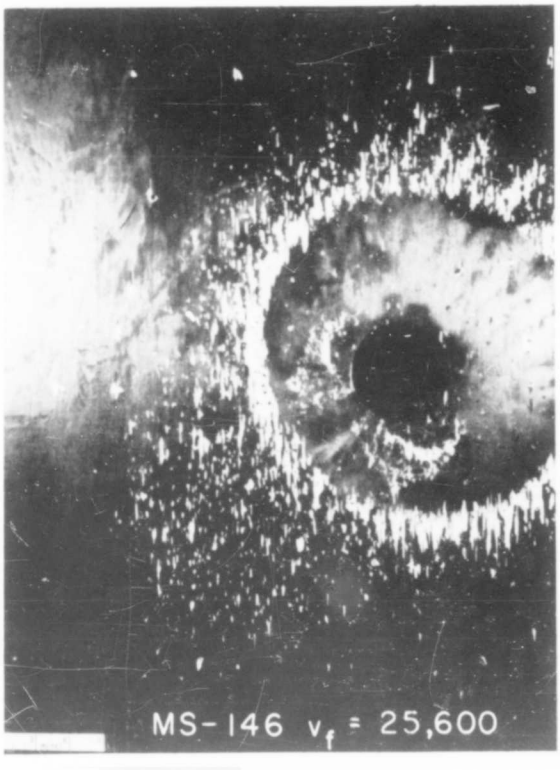

Figure 10.- Concluded.

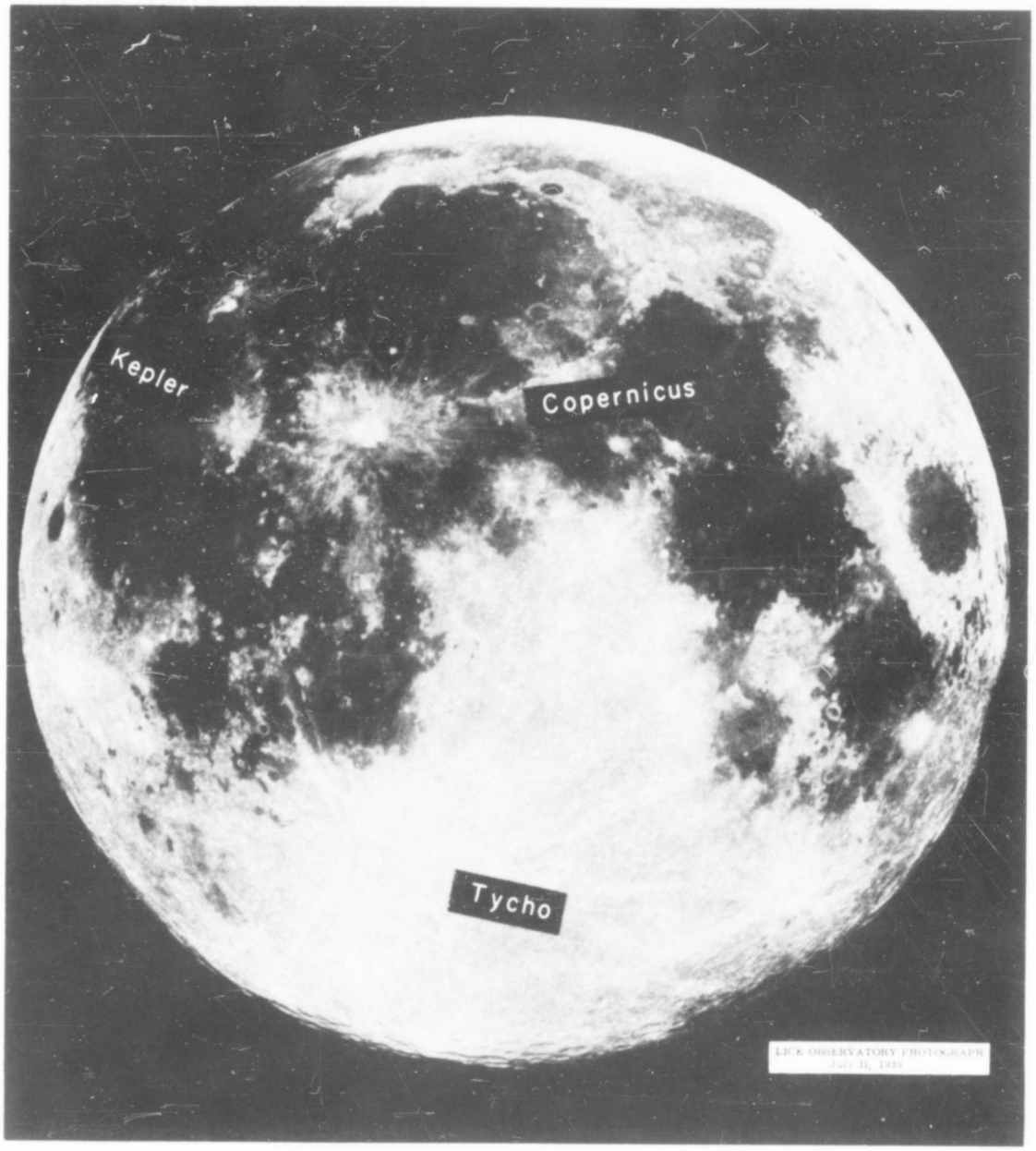

A-27995.2

Figure 11.- Ray patterns on the Moon.

NASA-Langley, 1962 A-566

NASA TN D-1210
National Aeronautics and Space Administration.
MEASUREMENTS OF MOMENTUM TRANSFER FROM PLASTIC PROJECTILES TO MASSIVE ALUMINUM TARGETS AT SPEEDS UP TO 25,600 FEET PER SECOND. B. Pat Denardo. March 1962. 30p.
OTS price, $0.75.
(NASA TECHNICAL NOTE D-1210)

Momentum transfer during impact at speeds from essentially 0 to 25,600 feet per second was measured by a simple ballistic pendulum. The change in mass of the target was also obtained, as were penetration data for this combination of materials. During the course of this experiment some interesting features of impact were observed; namely, crater formation and ejected spray patterns.

Copies obtainable from NASA, Washington

I. Denardo, Billy Pat
II. NASA TN D-1210

(Initial NASA distribution:
25, Materials, engineering;
52, Structures.)

NASA

NASA TN D-1210
National Aeronautics and Space Administration.
MEASUREMENTS OF MOMENTUM TRANSFER FROM PLASTIC PROJECTILES TO MASSIVE ALUMINUM TARGETS AT SPEEDS UP TO 25,600 FEET PER SECOND. B. Pat Denardo. March 1962. 30p.
OTS price, $0.75.
(NASA TECHNICAL NOTE D-1210)

Momentum transfer during impact at speeds from essentially 0 to 25,600 feet per second was measured by a simple ballistic pendulum. The change in mass of the target was also obtained, as were penetration data for this combination of materials. During the course of this experiment some interesting features of impact were observed; namely, crater formation and ejected spray patterns.

Copies obtainable from NASA, Washington

I. Denardo, Billy Pat
II. NASA TN D-1210

(Initial NASA distribution:
25, Materials, engineering;
52, Structures.)

NASA

NASA TN D-1210
National Aeronautics and Space Administration.
MEASUREMENTS OF MOMENTUM TRANSFER FROM PLASTIC PROJECTILES TO MASSIVE ALUMINUM TARGETS AT SPEEDS UP TO 25,600 FEET PER SECOND. B. Pat Denardo. March 1962. 30p.
OTS price, $0.75.
(NASA TECHNICAL NOTE D-1210)

Momentum transfer during impact at speeds from essentially 0 to 25,600 feet per second was measured by a simple ballistic pendulum. The change in mass of the target was also obtained, as were penetration data for this combination of materials. During the course of this experiment some interesting features of impact were observed; namely, crater formation and ejected spray patterns.

Copies obtainable from NASA, Washington

I. Denardo, Billy Pat
II. NASA TN D-1210

(Initial NASA distribution:
25, Materials, engineering;
52, Structures.)

NASA

UNCLASSIFIED